Presented at (e-e- 1997): The Electron-Electron Linear Collider Workshop
Santa Cruz, CA, September 4-6, 1997

LIMITATIONS IMPOSED BY BEAM-BEAM EFFECTS AND THEIR REMEDIES

J.E. SPENCER*
Stanford Linear Accelerator Center
Stanford University, Stanford, CA 94309, USA

Effects that limit the luminosities of a general purpose linear collider or GLC capable of $\vec{e}^{\pm}\vec{e}^{\pm}$, $\vec{\gamma}\vec{e}^{\pm}$ and $\vec{\gamma}\vec{\gamma}$ incident channels are discussed together with potential mitigations. The relative characteristics of such channels and their luminosities are predicted based on differing assumptions – including those for the current configurations for the NLC at $\sqrt{s}_{\rm ee}$= 0.5 and 1.0 TeV. Disadvantages related to the increased complexity of linear colliders can be offset by broader design constraints that seek to optimize the generalized luminosity. Decreased disruptions and bunch charges are effective and can be used in combination with feasable charge compensation schemes to predict higher luminosities and power conversion efficiencies. The incremental costs of additional channels is modest compared to the cost of any one by itself or potential gains in the integrated luminosity.

1. Introduction

In the first e^-e^-workshop[1] we noted that it was useful to look at $\vec{e}^-\vec{e}^-$ because electrons would be used to produce the other channels and because $e\gamma$ and e^-e^- collisions could provide new physics at SLC energies[2] far in advance of any NLC or GLC that might be built. Further, because the beam dynamics of the e^+e^- channel had been verified reasonably well at the SLC and studied further for the NLC at higher energies,[3] work concentrated on determining the achievable luminosities in the other channels in a way that was consistent with what was thought to be achievable for the e^+e^- channel. A generalized luminosity was defined and while the production of e^+ and especially $\vec{e}^+$ was an important distinguishing complication for e^+e^-, the more evident difference with e^-e^- resulted from beam-beam effects rather than any direct limit on achievable bunch intensities. A typical result, first presented in Refs. 3 & 4, was about a factor of three in luminosity between these channels due to the strong disruption intentially imposed on e^+e^-.

We begin by reviewing past results up to the present to motivate the important parameters of the problem as well as to motivate possible changes. We conclude with what we think are the most productive approaches from the perspective of a GLC facility. Although the basic cost of any next generation linear collider will be large, the incremental costs incurred by making a GLC should be relatively modest. Further, the broader perspective should provide certain practical advantages for the e^+e^- channel as well.

*Work supported by the US Department of Energy, Contract DE-AC03-76SF00515.

2. Previous Results, Parameters and Scalings

The single, most important figure-of-merit for colliders is the total, integrated, usable luminosity. The generalized luminosity[4] was based on the observation that **all** colliding beam machines as well as **all** incident channels in any particular GLC can be expected to have a geometric luminosity that is proportional to the square of the colliding bunch currents (I^2 or N^2 or fN^2 or nfN^2 etc.). This disarmingly simple statement is quite easy to misinterpret and misuse.

2.1. *The Generalized Luminosity* $\mathcal{L}$

For gaussian incident bunches, $\mathcal{L}$, in terms of the particles in a single bunch N_B and the undisrupted, rms spot sizes $\sigma^*_{x,y}$ at the interaction point[a] is:

$$\mathcal{L} \;=\; \frac{f_T n_B N_B^2 H_D}{4\pi\sigma_x^*\sigma_y^*}\zeta \;\rightarrow\; \frac{f_T n_B N_B^2 \gamma H_D}{4\pi\epsilon_n\beta^*}\,\zeta \;=\frac{f_T n_B N_B^2\gamma}{4\pi\widehat{\sigma}^2}\,\zeta \;\propto\; \frac{P_b}{\widehat{\sigma}^2}\Big(\frac{\widehat{N}_B^2}{N_B}\Big)\zeta'$$

where n_B is the number of bunches in a train and f_T is the RF rep-rate (the number of bunch trains/s). The arrow implies round beams. The dimensionless parameter H_D is the luminosity 'enhancement' defined in terms of the geometric luminosity as $\mathcal{L}/\mathcal{L}_G$ when the efficiency factor ζ=1 (NB: $\zeta'\gg1$ is possible e.g. $\zeta'\rightarrow n_B$). The electron beam power $P_b\propto fnN$ while ϵ_n is the invariant emittance and β^* is the magneto-optical 'depth of field' at the IP equivalent to the Rayleigh range Z_R for lasers. β^* is closely linked to the bunch length at the IP ($\sigma_z^*=\sigma_z$).

From the expressions for $\mathcal{L}$ and P_b it appears feasible to increase $\mathcal{L}$ for constant P_b by increasing N and decreasing f or n until all particles are in a single bunch with n_B=f_T=1. Unfortunately, this is currently impractical because of emittance, energy spread and associated beamsstrahlung problems. For example, the average energy loss from beamsstrahlung based on using unperturbed, gaussian bunches is:

$$\frac{\Delta E}{E} \;=\; \frac{8}{21}\frac{r_e^3 N_B^2\gamma}{\pi^{1/2}\sigma_z}\Big(\frac{2}{\sigma_x^*+\sigma_y^*}\Big)^2\big(1+(1.5\Upsilon)^{2/3}\big)^{-2}\;.$$

This varies mainly as N^2/σ^2, similarly to $\mathcal{L}$, and shows why one can't arbitrarily increase N or decrease σ quite apart from other practical limitations. The last term is a quantum efficiency factor[6] that varies rather slowly between 0$\rightarrow$1 where 1 implies a purely classical regime. Υ is a QED invariant measure of the beam induced field strength that drives the beam-beam interaction[4].

The longitudinal variables σ_z, n_B and f_T will be discussed later with some new transverse variables (n_x, n_y) that count the 'accelerators' in a cellular, matrix-like structure. n_q=1 or 2 will give the number of charge species in N_B. A simplified example using silicon, integrated-circuit technology will be used to illustrate some charge compensation options that can circumvent the beamsstrahlung constraint that was just discussed. The generalized luminosity with the new variables is:

$$\mathcal{L} \;=\; \frac{n_x n_y}{n_q}\frac{f_T n_B (N_B n_q)^2 H_D}{4\pi\sigma_x^*\sigma_y^*}\zeta \;=\; \frac{n_x n_y}{n_q}\frac{f_T n_B (N_B n_q)^2 H_D}{4\pi\sigma_x^{*2} R}\;\zeta \;= n_x n_y n_q\frac{f_T n_B \widehat{N}_B^2}{4\pi\widehat{\sigma}_x\widehat{\sigma}_y}\zeta'\;.$$

[a] We understand these to be the predicted rms sizes based on high order optical simulations[5]

This is a good example of why we specifically avoided labels on the luminosity $\mathcal{L}$ such as $\mathcal{L}_{ee}$ or on the number of electrons in a bunch N_B. If we take n_x=2n_y=2 and accelerate equal bunches of e^+ and e^- we then expect:

$$\mathcal{L}(n_x{=}2,n_y{=}1,n_q{=}2){=}4\mathcal{L}(n_x{=}1,n_y{=}1,n_q{=}1){=}\mathcal{L}(e^-e^-){+}2\mathcal{L}(e^+e^-){+}\mathcal{L}(e^+e^+)$$

assuming perfect alignment and charge compensation. Clearly, higher luminosities are possible in any number of conceivable configurations as will be discussed later.

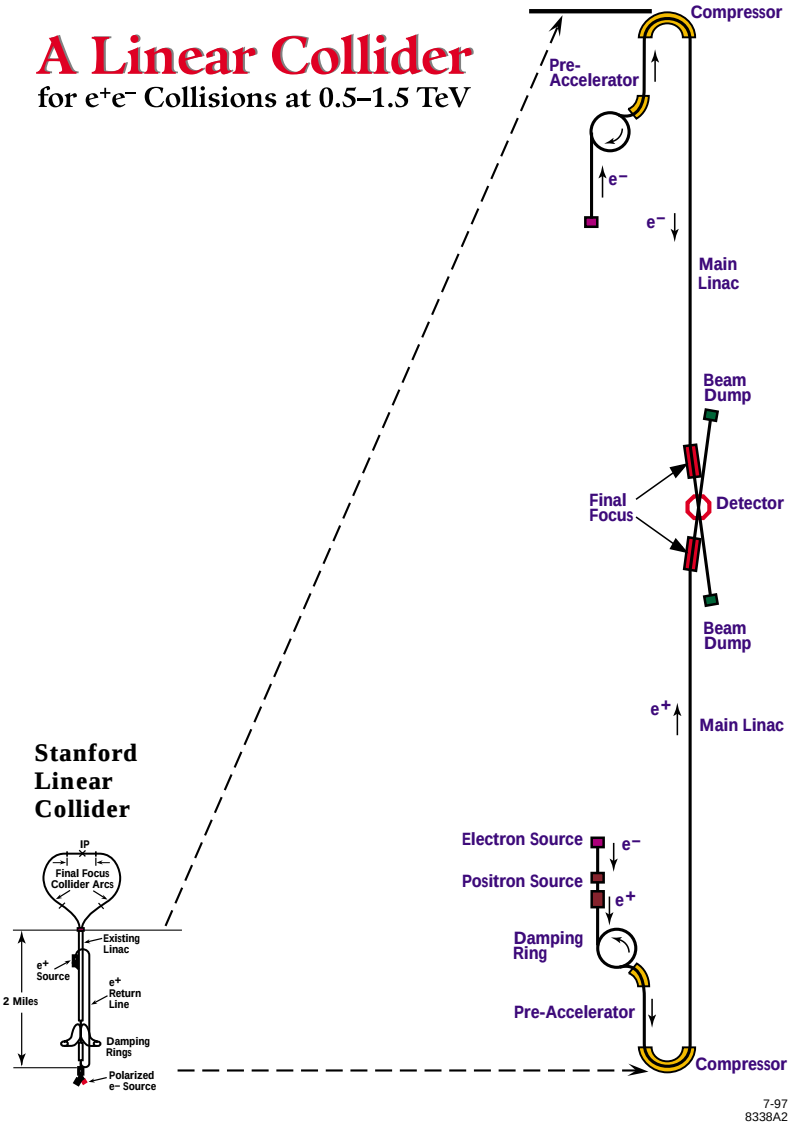

Fig. 1: The Next Generation e^+e^- Linear Collider NLC discussed in Refs. 3 & 4.

2.2. *A Summary of Previous Results and Conclusions*

Fig. 1 shows the archetypal second generation e^+e^- Next Linear Collider[3] relative to the SLC. This layout was the basis for all of the calculations discussed in Ref. 4.

We made the conservative assumption that any practically achievable e^- beams for the NLC e^+e^- designs would also be available for e^-e^-. The results of that assumption for these two channels were summarized in Table I of Ref. 4 which is partially excerpted here as Table II in Appendix A.

The previous results for 250 GeV unpolarized incident beams are summarized in Table I that gives the overall characteristics and expected luminosities for a nominal 250×250 GeV^2 ($\sqrt{s}_{ee}\equiv$500 GeV) GLC. $\langle s_\pm\rangle/s_{ee}$=0.97 for e^+e^- with an effective rms energy spread in each outgoing beam of $\delta_{\rm E}$=6.5%. Similarly, for the γ beam(s) we have $\langle s_{\gamma\gamma}\rangle/s_{ee}$=0.75 with $\delta_{\rm E}$=6.4% in each beam. The "less-than" sign in the Table is based on a mass shift in the strong laser conversion field that makes the effective electron mass heavier as well as the linear threshold for pair production. We note that if we were to use polarized electrons, we would expect to more than double the $e\gamma$ and quadruple the $\gamma\gamma$ luminosities (depending on the degree of electron polarization) or if we increase the γ energy spread, we can almost double the e^+e^- luminosity in the $e\gamma$ channel if we also reduce the separation distance between the conversion point (CP) and the interaction point (IP) sufficiently to insure that all of the produced photon energies overlap the electrons at the IP.

Table I: Achievable luminosities for a GLC using 250(500) GeV unpolarized, electrons based on NLC designs.[3,4] The integral is over one Snowmass year.

Incident Channel	$\mathcal{L}$ [10^{33}/cm^2 s]	$\int\mathcal{L}$dt [fmb^{-1}]	Threshold Energy	Comments
e^+e^-	6(13)	60	$\sqrt{s_{ee}}$	Pinch Enhanced
e^-e^-	2.3(4.5)	23	$\sqrt{s_{ee}}$	AntiPinch/Polarization
$e^\pm\gamma$	≥1	≥10	$< 0.91\sqrt{s_{ee}}$	$\sqrt{s}$ Discovery Advantage
γ-γ	≥0.1	≥1	$< 0.83\sqrt{s_{ee}}$	Backgrounds

Other results and conclusions that don't require too many caveats or reservations are itemized below:

- A general expression for the luminosity was shown to be consistent with all the beam species of potential interest for a linear collider.
- The most important parameter to optimize is the generalized luminosity $\mathcal{L}$ but this is overconstrained.
- It depends on essentially[7] three quantities: the average, primary beam power; the average rms bunch sizes at the IP when the beams are in collision; and the average number of particles in the bunches that are to be collided with those sizes.

- There are always ways to increase $\mathcal{L}$ by increasing the beam power P_B. Some are much better than others e.g. via f_T and/or n_B rather than N_B.
- Likewise, to obtain the same nonresonant event rate at twice the energy costs a factor of 2^4 more power for an equivalent storage ring when both collider types are operating at their respective beam-beam limits.
- It pays to optimize the generalized luminosity $\mathcal{L}$ because:
    1. The combination of different incident channels and polarizations provides unprecedented control of quantum numbers such as channel spin.
    2. Such "knobs" allow multiple, independent experiments for a broad range of final states.
    3. Such "knobs" allow these experiments to be optimized in various ways such as eliminating allowed final states that produce strong backgrounds.
    4. It is useful to shape the bunch charge distribution in all channels.
    5. It is necessary to employ crab cavities in all channels without charge neutralization.
    6. It is useful to be able to vary the bunch length in all channels.
- The beam-beam interaction in the e^+e^- channel is inherently stabilizing whereas in e^-e^- it isn't. Because $H_D \leq 0.5$ for the e^-e^- and $H_D \geq 1.4$ for e^+e^-, it is clear that without some form of field compensation scheme the best we expect for $\mathcal{L}(e^-e^-)$, using a conventional e^+e^- collider, is a factor of three or so less.
- However, discounting any stability problems for e^-e^-, the efficiency factor ζ should be better for e^-e^- than for e^+e^- and it could be seriously improved[8] by increasing both n_B and f_T when damping rings can be avoided for e^-.
- Strongly decreasing the geometric spot sizes or making them too asymmetric induces many practical problems and limitations even for e^+e^- such as jitter that varies proportional to the bunch charge and inversely with the smaller transverse spot size. This will reduce $\mathcal{L}$ and make it more difficult to monitor.
- Maxwell's equations limit our ability to simultaneously minimize σ_x^* and σ_y^* or β_x^* and β_y^* with normal lenses (*weak* focussing aside) but a charge neutralizing plasma or ion beam could make e^-e^- approach e^+e^- luminosity. However, the required densities in both cases appear too large to be practical.
- A major distinction between e^-e^- and the other channels is that reasonably large disruptions for pinch enhancement in e^+e^- and for dispersal of the low energy Compton electrons in the γ channels are thought necessary.
- Thus, the beam-beam disruption can be used as a strong focusing (or defocusing) lens in the transverse direction to influence luminosity but also to improve detector backgrounds and occupancy rates.

- The luminosity enhancement distribution $H_D(z)$ is pushed forward or backward depending on the relative sign of the charges of the colliding beams (sign of the equivalent lens) and the distribution is either widened or narrowed and may even modulate longitudinally.

2.3. *The 'longitudinal' Parameters*

Because the bandwidth of the control system and the stability of the accelerator and its various subsystems relates more to the RF rep-rate f_T than to the bunch number n_B, a practical solution appears to be multibunch trains to partition the total charge/pulse into a more continuous flow during each RF pulse. This improves the overall wall plug-to-beam power conversion efficiency and allows a higher RF repetition rate for a given power consumption. Increasing n_B clearly improves RF to beam power efficiency:

$$\eta = \frac{e n_B N_B E_{RF}}{W'} \equiv \frac{P_b}{P_{RF}} \ .$$

E_{RF} is the accelerating field and W' is the cavity energy per unit length. Notice that η is independent of f_T and the beam conversion and collision efficiency ζ but implies that higher RF frequencies f_{RF} would be useful.

Because the beamsstrahlung loss goes inversely with bunch length it is tempting to increase σ_z to allow larger N_B but this is limited both by β^* at the IP as well as the disruption D as discussed in the next section. Also, if N_B becomes too large one expects an increased energy spread between the head and tail that has to be compensated together with other associated wake field effects.

Thus, most current designs propose to accelerate several bunches per RF pulse with a lower N_B than for the SLC to improve energy conversion efficiency and average luminosity[8]. For a wall plug-to-RF efficiency of >30 %, the required wall plug power is 100 and 200 MW for the two energies labelled 'A' in Appendix A. Without efficient energy recovery or new acceleration techniques it is difficult to see how to further improve this significantly. Although the actual implementation of the improvement with n_B has not been tested we think that the next improvement may come with the transverse variables n_x and n_y.

2.4. *The Beam-Beam Interaction and 'Disruption' D*

The beam-beam interaction couples the particle detector to the accelerator and further constrains the usable luminosity through the backgrounds and occupancy rates. Again, assuming unperturbed gaussian bunches at the IP, the linearized, equivalent, beam-beam focal length[9] f is:

$$\frac{1}{f_{x,y}} = \pm \frac{2 N_B r_e}{\gamma \sigma_{x,y} (\sigma_x + \sigma_y)} \equiv \frac{D_{x,y}}{\sigma_z} \equiv \frac{\theta_D}{\sigma_{x,y}} \ .$$

θ_D is a characteristic angle for the full-energy, primary, disrupted particles. $\sigma_{x,y}/\sigma_z$ is called the diagonal angle θ_d and equals θ_D when $D_{x,y}$=1. The $\pm$ sign implies focusing(+) for e^+e^- and defocusing(-) for e^-e^-.

When the crossing angle $\theta_c > \theta_d$ one needs crab-crossing cavities.[b] Although D should clearly enhance the luminosity in the e^+e^- channel, D (and θ_D) are directly related to the beam-beam strength parameter (tune spread) in storage rings[12] ($\xi = \beta^*/4\pi f$) which characterizes their luminosity limits so we need to discuss them.

Typically, in the e^+e^- channel, the maximum disruption angle is in the horizontal with $\theta_{x,max} = \theta_D$ because the disruption parameter in the vertical is so large that one gets over focusing or a thick lens effect which gives an oscillatory motion whereas the focusing over the length of the beam in x is weaker but cumulative or more like a thin lens.[4] For e^-e^- the situation reverses and the vertical disruption angle dominates – more in line with our naive expectations. In either case, from Appendix A, one sees that θ_D is nearly an order of magnitude larger than for the incident beams e.g. for 250 GeV:

$$\theta_D = 257\mu\text{rad} \gg \sigma^*_{x'} = \sigma^*_{y'} = 36\mu\text{rad}.$$

Thus, while D enhances the geometric luminosity for e^+e^-, it provides a serious challenge for the extraction line[11] and for e^-e^-.

Similarly, Υ, $\Delta E/E$ and δ_B, the final rms energy spread due to beamsstrahlung, all go proportionally to some power of $N_B/\sigma^*_x(1+\text{R})$ with $\text{R} \equiv \sigma^*_y/\sigma^*_x$, the beam's unperturbed aspect ratio at the IP. Although $\Upsilon \lesssim 0.3$ is a typical limit to control beamsstrahlung intensity and pair backgrounds there is no consensus. Nevertheless, both observations and simulations for both storage rings and linear colliders have shown limits on the indiscriminate scaling of D related to the strong, nonlinear, nonconservative nature of the beam-beam interaction. Fortunately, representative calculations and models show that large D's are not necessary even for e^+e^-.

3. Some General Scaling Considerations

It is important to understand how RF acceleration developed before we can hope to understand whether it is relevant for the next generation of high energy machines or to determine what the next viable alternative might be. Further, it is important to know how the above variables scale with energy given the usual criterion that we want $\mathcal{L}$ to scale with $s(=4E_b^2)$. If $\mathcal{L}$ at $s_\circ$ is $\mathcal{L}_\circ$ we would like

$$\mathcal{L}(s) = \mathcal{L}(s_\circ)\left(\frac{s}{s_\circ}\right) = \mathcal{L}_\circ\left(\frac{\lambda_\circ}{\lambda}\right)^2$$

where λ is an equivalent length variable. Another possible constraint on N_B that becomes especially important for e^-e^-, where we would like to avoid the limitations imposed by damping rings is the scaling of normalized emittance with bunch charge i.e. in the region of interest here: $\epsilon_n[\mu\text{m}] \approx N_B[\text{nC}]$. This gives

$$\mathcal{L} \;=\; n_x n_y n_q \frac{f_r n_B N_B^2 \gamma H_D}{4\pi\beta^*_x \epsilon_{n,x} R}\;\zeta \;\propto\; \frac{P_b H_D}{\beta^*_x R}\left(\frac{N_B}{\epsilon_{n,x}}\right) = \; P_b\left(\frac{H_D}{\sigma^*_y}\right)\left(\frac{\sigma^*_x}{\beta^*_x}\right)\left(\frac{N_B}{\epsilon_{n,x}}\right) .$$

[b] We note that for multibunch operation ($n_B > 1$) we need to introduce crossing angles[10,3] at the IR and design the final focus quadrupoles and beamline[11] to minimize the effects of the outgoing, disrupted beam on the incoming beam or detector when D is large i.e. $D > 1$.

Table II in Appendix A gives some examples that are consistent with this and check the consistency of completely independent calculations. They show how one can obtain a more consistent approach to e^+e^- and e^-e^- without doing damage to e^+e^-. There are still just three basic parameters because we introduced n_x and n_y to increase $\mathcal{L}$ in a way that optimizes power for P_b. We note that β_x^*, N_B and $\epsilon_{n,x}$ scale as λ and f_T, P_b, f_{RF} and the accelerating gradient scale inversely with λ.

4. New Acceleration Techniques and Charge Compensation Schemes

Although there are several approaches being pursued at present, one that appears well suited to solve a number of problems for a GLC and especially for e^-e^- is vacuum laser acceleration. The basic physics for a single acceleration cell[13] is shown in Fig. 2.

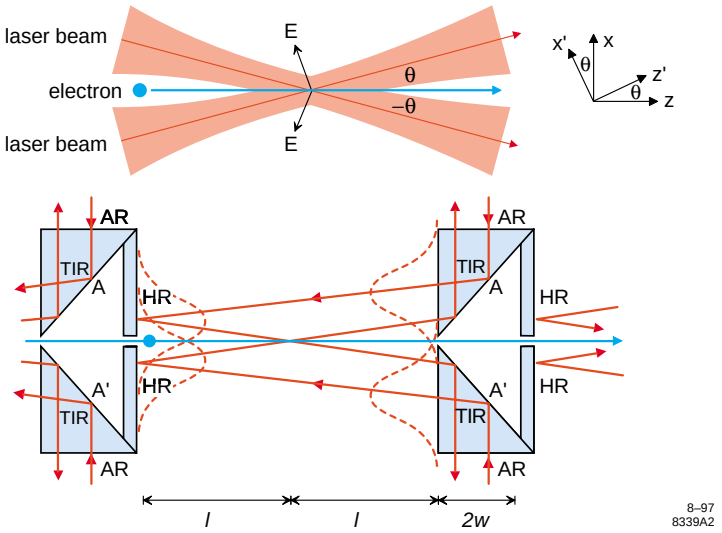

Fig. 2: Schematic layout for a single, discrete laser acceleration cell.

A single laser beam is split and the two halves are then propagated and crossed in vacuum at an angle $|\theta|$ with the electron beam that follows along the central axis (z) of the cell. The original laser beam is transversely polarized in the crossing plane (xz) and the two halves are π out of phase at the crossing point such that the (strong) transverse components of the field interfere destructively ($E1_x$+$E2_x$=0) while the longitudinal components add to provide a net acceleration. Assuming gaussian laser beams, the paraxial, on-axis, accelerating field is

$$E_z \approx -\sqrt{\frac{\eta_V P_L}{\pi}}\frac{4\theta w_\circ}{w^2}\exp\left(\frac{z^2\theta^2}{w^2}\right) \times \exp i\psi$$

where η_V is the vacuum wave impedance, P_L is the laser power and ψ is made of three phases including the Guoy phase advance[14] ψ_G=2tan(z/Z_R). For a gaussian field, it gives a π phase advance from $z=-\infty$ to $z=\infty$. To obtain net acceleration, it follows that there must be at least *one* boundary to terminate the field at $|z|<Z_R$.

If $w_\circ$ is the waist size and $Z_R{=}\pi w_\circ^2/\lambda$ is the Rayleigh range, then the distribution that we have to match to the particle beam is:

$$w^2 = w_\circ^2[1 + (\frac{z^2}{Z_R^2})] \ .$$

The other phases relate to wavefront curvature and the phase relative to the particle bunch.

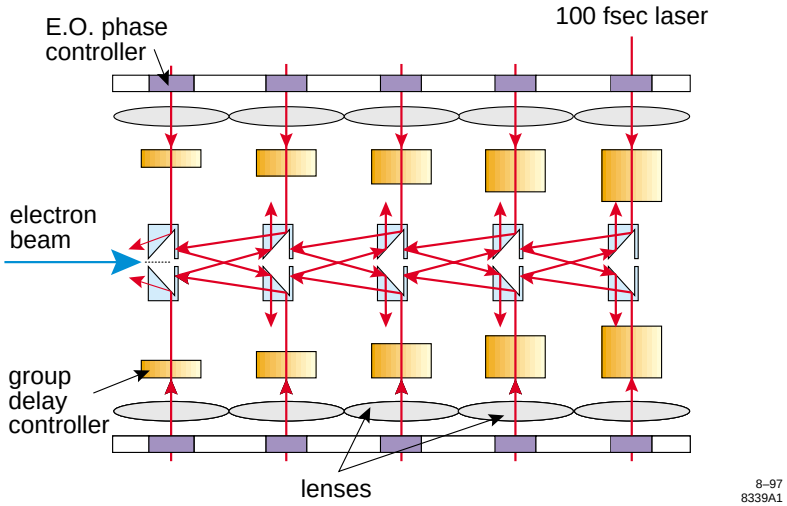

Fig. 3: Schematic layout for a discretized, multicell laser accelerator.

Fig. 3. shows the basics required for the corresponding multicell accelerator. Light from a high power, diode pumped laser is split into several components prior to the split shown in Fig. 2. To maintain the overall phase coherence between cells, an electro-optical phase element is included to control the overall phase and a group delay element to match individual cells to the electron beam in each cell. A high energy accelerator will presumably require many such multicell structures and coupled high power laser sources.

While the discrete structures shown in Figs. 2-3 are useful for testing[15] various aspects of vacuum acceleration, they appear impractical for large scale fabrication. Although the experiment is quite interesting in what it proposes to test, it will not be discussed except as it relates to a multicell accelerator such as discussed above. Of interest here, however, is that such high frequency structures, whatever their specific form, are naturally suited to using smaller, lower emittance bunch charges as advocated above.

Fig. 4 shows a more practical example for an actual accelerator that is being studied by Tomas Plettner of the LEAP collaboration. In this example, showing a planar view of a structure that is intended to extend considerably above and below the plane, linearly polarized light enters on one side and exits on the other at the Brewster angle where it can then be used in a number of ways.

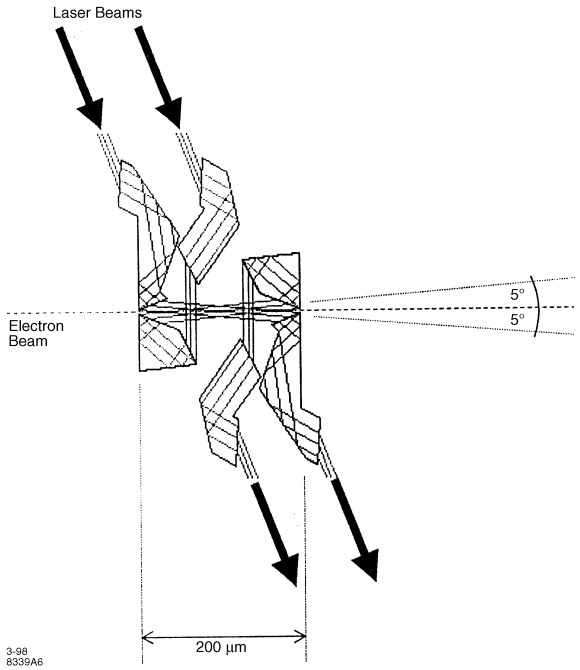

Fig. 4: A more integrated example of a single, laser cell.

For example, because it is intended to be fabricated using integrated circuit techniques, one can as easily make an array of these as make a single structure. One example is shown in Fig. 5. The spacing between linear arrays can contain active phase control elements such as one would need if they intended to use it for arbitrarily charged beam species. Although this suggests a very significant research development the various technologies that are required are available now at reasonable costs and are also improving rapidly. This can not be said for the next generation RF structures either in terms of their fabrication technologies or their power sources.

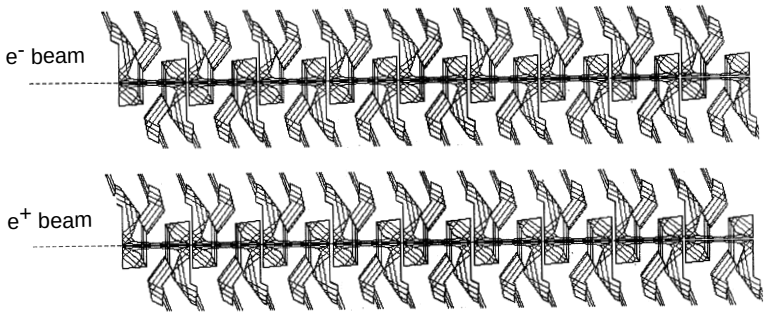

Fig. 5: Layout for a multicell structure for simultaneous e^+e^- or e^-e^- acceleration.

5. Problems and Considerations for Multibunch/Multibeam Operation

Although it was not our goal to discuss acceleration schemes, our approach to the beam-beam problem was to question the prevailing criteria based on the e^+e^- channel. Originally, 'cylindrical' beams were thought best because 'disruption' was considered bad. The reverse is now true but we have tried to show that neither is necessary. All channels could benefit if charge compensation was possible. Several ways to do this have been considered.[8,4] Plasmas or ion beams require densities comparable to the beam(s) to be compensated which in our case is quite high and quite difficult. Our conclusion is that it is probably impractical unless the other beam is comparable in all respects but charge. This has the added advantage that it would then produce luminosity rather than backgrounds. Charge compensation is best accomplished when the beams to be combined are spatially close.[8] While the proposed method is good, there are still combination and transport problems of the beams to the IP and their subsequent extraction and disposal.

Previously, a chicane was developed for the NLC extraction line that provided both diagnostics and disposal for *all* charge species that exited the IP including the neutrals and primary beam.[11] The beams were analyzed in the first half of the chicane and then recombined for disposal in a common dump. The same type of system is relevant here for both purposes. In the notation of Ref. 11, the first half of the exit chicane is the beam combiner for parallel, incident, oppositely charged beams when they are separated by Δx:

$$\frac{\Delta x}{2} = 2\rho_B(1-\cos\theta_B) + L_1\tan\theta_B \approx \rho_B\theta_B^2(1+\frac{L_1}{L_B})$$

where θ_B is the bend angle for one rectangular dipole of length $L_B = \rho_B \sin\theta_B$ and L_1 is the separation between bends. This combination requires a minimum distance

$$L_{min} = 2\rho_B \sin\theta_B + L_1 \ .$$

We need to know what such systems do to the beam sizes at the IP e.g. what is the emittance growth from synchrotron radiation and what are the higher order spot sizes due to the transport. For this we need the magneto-optics for the beams and their characteristics. From Figs. 4-5 and the configuration labelled '1000 SC' in Table II, we have for the input at the middle of the chicane

$$\epsilon_x = \epsilon_y = 1.02\times10^{-13} \text{ m}; \quad \beta_x = \beta_y \equiv 1 \text{ m} \ \Rightarrow \ \sigma_x = \sigma_y = 0.32 \ \mu\text{m} \ .$$

Because we already know[11] η_x and η_y, we can define δ_B from an assumed limit of 10 % growth in the spot size from the incident energy spread:

$$\eta_x = \frac{\Delta x}{2} = 250 \ \mu\text{m}, \eta_y = 0 \ \Rightarrow \ \delta_B \equiv 0.10\frac{\sigma_x}{\eta_x} \ = \ 0.013 \ \%.$$

Notice that this is the input beam and not the beamsstrahlung broadened output result in Table II predicted for conventional, non charge compensated e^-e^-. Because

this is reasonable, our next concern is the growth of energy spread and emittance in the transport chicane dipoles (or other included optics) i.e. whether we can maintain the assumed values. From the chicane dipoles we expect[16]

$$(\delta_B^*)^2 \geq \left(\frac{55 r_e \lambda\!\!\!^{-}_c}{12\sqrt{3}}\right)\frac{\gamma^5\theta_B^3}{L_B^2} \leq 10^{-2}\times(\delta_B)^2 = 10^{-4}\left(\frac{\sigma_x}{\eta_x}\right)^2 = 4\times 10^{-4}\left(\frac{\beta_x\epsilon_x}{\Delta x^2}\right)$$

for zero input spread ($\delta_B \equiv 0$). With this we find

$$(\gamma\theta_B)^5 \;\leq\; 3.5\times 10^{26}\times 10^{-4}(\beta_x[\mathrm{m}]\epsilon_x[\mathrm{m}])$$

For 500 GeV, this gives $\theta_B \leq$83 μrad. Constraining the emittance growth to 10 % of Table II puts a slightly stronger limit of $\theta_B \leq$78 μrad. Since $L_B \approx \Delta x/2\theta_B$, this implies $L_B \geq$3.2 m and an induction field B$\leq$400 G. A 'momentum compaction'[11] of 13 nm implies insignificant bunch lengthening. Higher order effects suggest the focusing elements be part of the integrated circuit via laser ponderomotive effects, crystal channeling or 'conventional' currents or materials that can be quite strong.

6. Conclusions

We summarized our previous results in Table I noting that while e^+e^- has pinch enhancement, e^-e^- is cleaner than the other channels because it is severely limited by charge and lepton number conservation which provides unique opportunities.[17] From the perspective of all of these channels, the 'disruption' is an apt description that has caused considerable confusion and tended to drive high energy accelerator development toward higher bunch charges rather than more bunches. We tried to show that this isn't necessary even for e^+e^- and is even inconsistent with higher energies and their increased complexity.

The alternative of significantly lower bunch charges and more bunches offers substantial improvements in both power utilization and usable luminosity. We showed why $\mathcal{L}$ can be increased by increasing n_B without increasing the required RF power and, by analogy, further increased by implementing two new variables n_x and n_y. We then gave what may be a practically viable way to achieve this that also solves a major difficulty with increasing n_B using conventional RF. Extending RF frequencies significantly higher is inconsistent in many ways with its original rationale until there are more natural fabrication methods. By the same argument, one tends to dismiss the possibility of laser acceleration at even higher frequencies even though it can use the very well developed fabrication technologies for silicon integrated circuits and the rapidly developing field of semiconductor laser diodes.

We demonstrated that an accelerator such as assumed for the next generation of linear colliders is practical using small, laser based structures. Further, because of the wavelength, one can infer that it should be optimally efficient and able to use high values of $n_x \gg n_y$ with $n_y \gg$10. The luminosity might then be orders of magnitude higher for comparable wall-plug powers. With sufficiently decreased disruption, one can pass to the proportionality limit of $\mathcal{L} \propto n_B^2$. Such changes could restore the exponential growth in energy that was enjoyed in the past.

7. Acknowledgements

The author wishes to thank Clem Heusch and Nora Rogers for a productive and enjoyable workshop. He also thanks members of LEAP for a considerable amount of fun work and the opportunity to learn more about lasers. Especially, he thanks Nora, Terry Anderson and Rachel Denning for their indispensable help in realizing this work and finally W.K.H. (Pief) Panofsky whose presence and participation set an impressive example for the other participants. This work was supported by the U.S. Department of Energy under contract DE-AC03-76SF00515.

References

1. e-e- 1995: Proceedings of the Electron-Electron Linear Collider Workshop, Ed. C.A. Heusch, Santa Cruz, CA, Sept. 4-5, 1995. *Intl. J. Mod. Phys.***A11** (1996) 1523.
2. J.E. Spencer, Uses of a Prototype NLC/GLC, *Nucl. Inst. Meth.***A355** (1995) 1.
3. Zeroth-Order Design Report for the Next Linear Collider, May 1996, SLAC Report 474, LBNL-PUB-5424, UCRL-ID-124161.
4. J.E. Spencer, Beam-Beam Effects and Generalized Luminosity, *Intl. J. Mod. Phys.***11** (1996) 1675. See also SLAC-PUB-7051, January 1996.
5. K.L. Brown and J.E. Spencer, Non-Linear Optics for the Final Focus of the Single-Pass Collider, *IEEE Trans. Nucl. Sci.*, **NS-28** (1981) 2568.
6. K. Yokoya and P. Chen, Beam-Beam Phenomena in Linear Colliders, Proc's. Topical Course on Part. Accel's., LNP 400, Nov.7-14 (1990) 415.
7. See also: Robert H. Siemann, Linear Colliders: The Last Ten Years and the Next Ten, SLAC-PUB-6417, 1994.
8. J.E. Spencer, The SLC as a Second Generation Linear Collider, IEEE95CH35843, Proc's: 16th IEEE Part. Accel. Conf. and Intl. Conf. on High Energy Accel's., R. Siemann, Ed., Dallas, TX, (1995) 671.
9. Robert Hollebeek, Disruption Limits for Linear Colliders, *Nucl. Inst. Meth.***184** (1981) 333.
10. R.B. Palmer, Prospects for High Energy e^+e^- Linear Colliders, *Ann. Rev. Nucl. Sci.* **40** (1990) 529.
11. J. Spencer, J. Irwin, D. Walz and M. Woods, The SLAC NLC Extraction and Diagnostic Line, IEEE95CH35843, Proc's: 16th IEEE Part. Accel. Conf. and Intl. Conf. on High Energy Accel's., R. Siemann, Ed., Dallas, TX, (1995) 671.
12. A.W. Chao, Beam-Beam Instability, in *Physics of High Energy Particle Accelerators*, AIP Conf. Proc. No. 127 (1985) 202.
13. Y.C. Huang, D. Zheng, W.M. Tulloch, R.L. Byer, *Appl. Phys. Lett.*, 68 (1996) 753.
14. A.E. Siegman, *Lasers*, Mill Valley, CA, 1986.
15. Y.C. Huang, T. Plettner, R.L. Byer and R.H. Pantell (Ginzton Labs); R.L. Swent and T.I. Smith (HEPL), J.E. Spencer, R.H. Siemann and H. Wiedemann (SLAC), The Physics Experiment for a Dielectric Laser-Driven Electron Accelerator, Proc. 19th FEL Conf., Beijing, PRC, August 1997.
16. M. Sands, The Physics of Electron Storage Rings, SLAC Report–121, 1979. R.H. Helm, M.J. Lee,P.L. Morton, M. Sands, Evaluation of SR Integrals, IEEE PAC (1973) 900.
17. Clemens A. Heusch, e^-e^- Physics at an e^-e^- Collider, Workshop on Gamma-Gamma Colliders, *Nucl. Inst. Meth.***A355** (1995) 75; *Intl. J. Mod. Phys.***11** (1996) 1523.
18. K. Yokoya, ABEL, A Computer Code for the Beam-Beam Interaction in Linear Colliders, *Nucl. Inst. Meth.***B251** (1986) 1 as well as Toshiaki Tauchi et al. *Part. Accel.***41** (1993) 29.

Appendix A – Achievable e^- Beams, Luminosities and Scalings

Table II, with the columns labelled 'A' from Ref. 4 for some currently preferred NLC configurations, compares the predicted channel luminosities for $\mathcal{L}_{e^\pm}$ and $\mathcal{L}_{e^-e^-}$. $\mathcal{L}_{Compton}$ and $\mathcal{L}_{\gamma\gamma}$ are secondary to the e^+e^- channel. $\mathcal{L}_{\gamma\gamma}$ is rather large because it includes contributions from real and virtual photons and the beamsstrahlung parameter Υ is fairly large. Parameters such as the number of electrons (or positrons) per bunch apply to both beams unless otherwise stated. Machine parameters that are not discussed such as l^*, the distance from the IP to the first quad, are the same as for 'A' in Table I (see Ref. 4). All calculations such as those with ABEL91[18] and our variants of it were checked by analytic calculations wherever practicable.

Table II: Beam-Beam effects for e^+e^- and e^-e^- at E_{cm}=500 and 1000 GeV. NLC configurations are labelled 'A' and (...) indicates analytic calculations.

$\sqrt{s}_{\rm NLC}$ [GeV]	500A	500SC	1000A	1000SC
$f_{\rm rep}$[Hz]	180		120	
n_B	90		90	
$N_B[10^9]$	6.5	0.80	9.5	0.80
$P_B/E_B \equiv n_B N_B f_{\rm rep} 10^{12}$	105.3	105.3	102.6	102.6
$\gamma\epsilon_x/\gamma\epsilon_y$ $[10^{-8}m]$	500/8	8/8	500/10	10/10
σ_x^*/σ_y^*[nm]	285.9/4.52	36.2/4.52	226.1/3.57	32.0/3.57
$\sigma_z[\mu m]$	100	100	125	125
β_x^*/β_y^*[mm]	8/0.125	8/0.125	10/0.125	10/0.125
$\mathcal{L}_G[10^{34}{\rm cm}^{-2}{\rm sec}^{-1}]$	0.42	0.41	0.96	0.57
$(\lvert D_x\rvert/\lvert D_y\rvert)$	0.090/5.70	0.626/5.01	0.132/8.33	0.507/4.53
θ_D [μrad]	(257)	(226)	(238)	(130)
Υ	(0.10)	(0.09)	(0.30)	(0.18)
$H_D \equiv \mathcal{L}_{e^\pm}/\mathcal{L}_G$	1.42	2.02	1.36	1.67
$\mathcal{L}_{e^\pm}[10^{34}{\rm cm}^{-2}{\rm sec}^{-1}]$	0.60	0.85	1.30	0.95
$\langle s\rangle/s_{\rm NLC}$	0.972	0.941	0.913	0.922
$s_{rms}/s_{\rm NLC}$	0.068	0.106	0.144	0.137
$\langle E_\circ - E_{in}\rangle/E_{in}$	0.032	0.054	0.103	0.073
$\delta_B \equiv (E_\circ)_{rms}/E_{in}$	0.065	0.097	0.142	0.121
$\mathcal{L}_{100}/\mathcal{L}_{e^\pm}$	0.376	0.299	0.195	0.287
N_γ/N_e	0.98	1.29	1.67	1.30
$\langle E_\gamma\rangle/E_\circ$	0.033	0.042	0.062	0.056
$\mathcal{L}_{Compton}$	0.23	0.41	0.80	0.45
$\mathcal{L}_{\gamma\gamma}[10^{34}{\rm cm}^{-2}{\rm sec}^{-1}]$	0.10	0.18	0.56	0.35
$H_D \equiv \mathcal{L}/\mathcal{L}_G$	0.55	0.52	0.47	0.54
$\mathcal{L}_{e^-e^-}[10^{34}{\rm cm}^{-2}{\rm sec}^{-1}]$	0.23	0.21	0.45	0.31
$\langle s\rangle/s_{\rm NLC}$	0.980	0.985	0.940	0.97
$\langle E_\circ - E_{in}\rangle/E_{in}$	0.031	0.025	0.095	0.041
$\delta_B \equiv (E_\circ)_{rms}/E_{in}$	0.064	0.056	0.138	0.084
$\mathcal{L}_{100}/\mathcal{L}_{e^\pm}$	0.396	0.449	0.215	0.408
N_γ/N_e	0.95	0.83	1.60	0.93
$\langle E_\gamma\rangle/E_\circ$	0.032	0.031	0.059	0.045